



Rapid Solidification of a Columnar Hexagonal Liquid Crystal

To cite this article: J. C. Géminard *et al* 1993 *EPL* **22** 69

View the [article online](#) for updates and enhancements.

Related content

- [Contact Angle Hysteresis on a Heterogeneous Surface: Solution in the Limit of a Weakly Distorted Contact Line](#)
J. Crassous and E. Charlaix
- [Pattern Formation during Mesophase Growth in Liquid Crystals](#)
S. Arora, A. Buka, P. Palffy-Muhoray *et al.*
- [Nonparabolic Dendrites of a Smectic Phase Growing into a Supercooled Nematic](#)
A. Buka and N. Éber

Recent citations

- [Phase-field model for front propagation in a temperature gradient: Selection and competition between the correlation and the thermal lengths](#)
V. Popa-Nita
- [Pattern Formation at the Nematic Smectic-B Interface](#)
Tibor Tóth-Katona *et al*
- [Pattern forming instabilities of the nematic smectic-B interface](#)
T. Tóth-Katona *et al*

Rapid Solidification of a Columnar Hexagonal Liquid Crystal.

J. C. GÉMINARD, P. OSWALD, D. TEMKIN(*) and J. MALTHÊTE(**)

*Laboratoire de Physique, Ecole Normale Supérieure de Lyon
46 Allée d'Italie, 69364 Lyon Cedex 07, France*

(received 19 October 1992; accepted in final form 1 February 1993)

PACS. 81.10F - Growth from melts.

PACS. 64.70M - Transitions in liquid crystals.

PACS. 64.70D - Solid-liquid transitions.

Abstract. - We have measured the molecular-attachment kinetic law for the interface velocity of the columnar hexagonal phase of the liquid crystal HET (hexaoctyloxytriphenylene) when it grows into its isotropic liquid. This law is linear and characterized by a kinetic coefficient $\mu(\theta) = \mu(1 + \varepsilon_6 \cos 6\theta)$. The coefficient μ is close to $130 \mu\text{m/s}/^\circ\text{C}$ and is independent of the impurity concentration. The anisotropy has been measured ($\varepsilon_6 \approx 5.6 \cdot 10^{-3}$) as well as the directions of maximal $\mu(\theta)$: they make a 30° angle with the directions of maximal surface energy $\gamma(\theta)$.

Recently, we have studied the growth of the discotic liquid crystal HET (2, 3, 6, 7, 10, 11-hexa-*n*-octyloxytriphenylene) [1] at dimensionless supersaturations less than 1. We have shown the existence of three growth regimes: a diffusive petal-shape regime at very small supersaturation, the dendritic regime at intermediate supersaturations and the dense branching regime at supersaturation close to 1. In this article, we examine what happens at supersaturation larger than 1. In this case, attachment kinetics are known to play an essential role.

Our goal is to show that it is possible to reach the limit of absolute restabilization and to measure accurately the kinetic coefficient and its anisotropy. Next, we shall discuss the physical origin of the kinetic process.

In order to observe the rapid solidification of the hexagonal mesophase, it was necessary to quench the samples. Briefly, the sample is first sandwiched between two 1 mm thick glass plates, one of which is coated with a conducting transparent ITO layer. The sample thickness, ranging between 2 and $20 \mu\text{m}$, is measured to about $\pm 0.2 \mu\text{m}$ on an optical bench with a Brace-Köhler compensator. This method is possible because the liquid crystal is birefringent. This sample is then placed in an oven whose temperature is controlled to about $\pm 3 \text{ mK}$. The temperature is chosen below the solidus temperature, because we are

(*) Permanent address: I. P. Bardin Institute for Ferrous Metals, 2 Baumanskaya, Str. 9/23, 107005 Moscow, Russia.

(**) Permanent address: Université de Paris-Sud, Laboratoire de Physique des Solides, Bât. 510, 91405 Orsay Cedex, France.

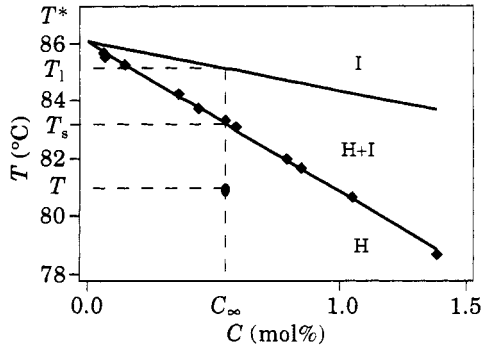


Fig. 1. - Experimental phase diagram, measured as described in ref.[2]. The impurity solute concentration has been estimated from the law of Van t'Hoff for dilute solution. H means hexagonal mesophase and I isotropic liquid. $T^* = 86.1$ °C is the extrapolated melting temperature of the pure HET. $K = 0.33$.

interested in working at supersaturation larger than 1. We recall that the supersaturation is defined to be⁽¹⁾

$$\Delta = \frac{T_l - T}{T_l - T_s}, \quad (1)$$

where T_s (respectively, T_l) is the solidus (respectively, the liquidus) temperature and T the actual growth temperature (fig. 1). In order to grow a germ, we send an electric impulse (typically 50 V during 0.1 s) through the conducting layer in contact with the liquid crystal. Its duration is chosen to be as short as possible, in order to melt the liquid crystal without appreciably heating the glass plates. Just after the impulse, the sample temperature decreases exponentially with an initial slope of about 10 °C/s. After a few seconds, the temperature of the sample is again equal to that of the oven. Because the rate of heterogeneous nucleation increases with the undercooling, germs often nucleate before the sample temperature is restabilized. For this reason, we record simultaneously the average sample temperature (obtained by measuring the temperature-dependent electric resistance of the ITO layer) and the times at which the different germs nucleate. In this way, it is possible to determine the actual supersaturation at which each germ has grown. Experimentally, it ranges between 1 and 14. The germs are also video-taped and then digitalized on a Macintosh II computer, in order to measure the front velocity as a function of the supersaturation. This method allows us to determine the temperature to ± 0.3 °C and the front velocity to about 1%. The main sources of errors are due to the smallness of the temperature coefficient of the conducting layer (40 m Ω /°C) and to the fact that the internal timer of the computer gives the time with a precision of only 0.2 s.

⁽¹⁾ The supersaturation, as we have defined it, is different from the chemical supersaturation Δ_c generally used, in particular in ref.[1,2]. The relationship between them is

$$\Delta_c = \frac{C_0 - C_\infty}{C_0(1 - K)} = \frac{\Delta}{(1 - K)\Delta + K},$$

where C_0 is the impurity concentration in the liquid at temperature T given by the liquidus line of the phase diagram.

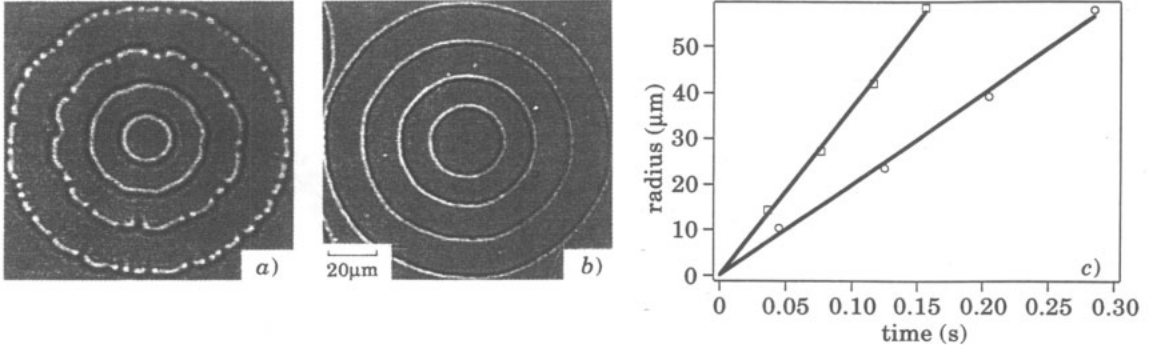


Fig. 2. – Two germs growing at different supersaturations *a*) at $\Delta = 3$, the front is locally unstable; *b*) at $\Delta = 5$, the front is perfectly stable up to the microscope resolution. On the other hand, its shape is slightly hexagonal. *c*) Radius *vs.* time. ○ for $\Delta = 3$, □ for $\Delta = 5$.

Figure 2 shows the growth in the basal plane (the molecular columns are perpendicular to the glass plates) of two germs at different supersaturations ($\Delta \approx 3$ and $\Delta \approx 5$) and the evolution of their radii as a function of time. In both cases, the front velocity is constant and depends only upon temperature. One notes also that the globally circular front is locally unstable at $\Delta \approx 3$, whereas no cellular structure is visible at large supersaturation. Thus, there exists experimentally a critical value Δ^* above which the front restabilizes. Experimentally, we find a value $\Delta^* \approx 4 \pm 2$ that is independent of the impurity concentration within our experimental errors (fig. 3). Note that this supersaturation defines the limit above which we no longer see cells within the resolution of the microscope. Therefore, the experimental value necessarily underestimates the true Δ^* . The phenomenon of «absolute restabilization» will be analysed in detail in a more complete publication. Figure 4 shows the front velocity V as a function of $T_s - T$: the different symbols represent samples of various impurity concentrations and thicknesses. Within the experimental errors, all these points lie on the same straight line as long as $\Delta > 1.5$:

$$V(\mu\text{m/s}) \approx 130(T_s - T)(^\circ\text{C}). \tag{2}$$

This is the signature of a linear kinetic law. The slope of this curve gives the kinetic coefficient $\mu \approx 130 \mu\text{m/s}/^\circ\text{C}$ ⁽²⁾. This coefficient, being independent of the impurity concentration, must be the same for the pure material. It characterizes the interface dissipation and by how much the system must be shifted from equilibrium in order to make the front grow at a given velocity.

One must, however, be cautious because the measured front velocity could be due to the latent heat release and its diffusion in the glass plates, rather than to kinetic effects. One can nevertheless reject this interpretation for two reasons. First, the front velocity is independent of the sample thickness over a large range. Second, it is possible to determine analytically the conditions under which thermal effects are negligible compared to

⁽²⁾ Recently, we argued that if the solid phase wets preferentially the glass plates, just measuring the meniscus velocity leads to overestimate the kinetic coefficient [3]. This wetting effect can be neglected in the opposite case, the measured coefficient being equal to the real one at large enough velocity. We have checked that in our system the liquid wets the plates better than the solid, with a contact angle near to 30° , so that no correction is necessary.

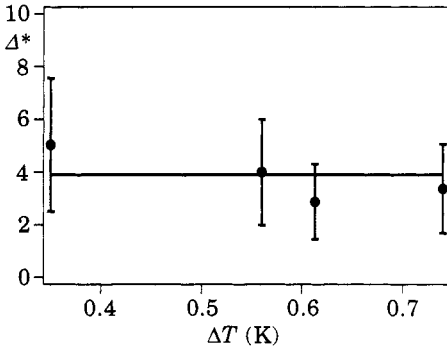


Fig. 3.

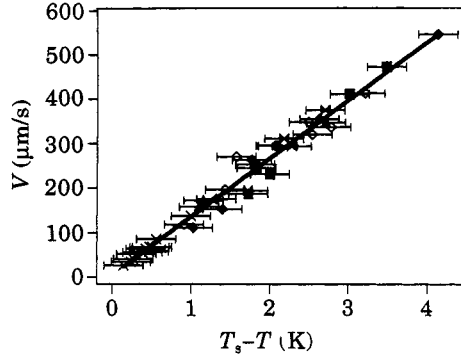


Fig. 4.

Fig. 3. - Supersaturation Δ^* ($\approx 4 \pm 2$) of absolute restabilization vs. the freezing range $\Delta T = T_i - T_s$.

Fig. 4. - Front velocity V vs. undercooling $T_s - T$: \times $\Delta T = 0.40$ K, \bullet $\Delta T = 0.30$ K, \blacktriangle $\Delta T = 0.35$ K, \blacksquare $\Delta T = 0.64$ K, \blacktriangleright $\Delta T = 0.74$ K, \diamond $\Delta T = 0.55$ K.

attachment kinetics. Indeed, the front is equivalent to a line source of heat propagating at velocity V in a medium of thermal conductivity κ (we assume that the conductivities of the substrate and of the sample are equal). The latent heat is negligible if the local overheating of the front is much smaller than the imposed undercooling:

$$T_i - T \ll T_s - T, \quad (3)$$

where T_i is the local interface temperature and T the temperature imposed far away (that we measure experimentally). An estimation of the heat flux from the interface gives $LV \approx \kappa(T_i - T)/d$. On the other hand, the velocity is given by the kinetic relation, namely $V = \mu(T_s - T_i)$. From these two relations, it follows that $(T_i - T)/(T_s - T) \approx 1/(1 + \kappa/Ld\mu)$. Thus, condition (3) is fulfilled if

$$\frac{Ld\mu}{\kappa} \ll 1, \quad (4)$$

where L is the latent heat per unit volume and d the sample thickness (see (1)). As expected, thermal effects decrease when latent heat, kinetic coefficient or sample thickness decrease and when the heat conductivity increases. Experimentally, $\kappa \approx 10^4$ erg/cm/s/K,

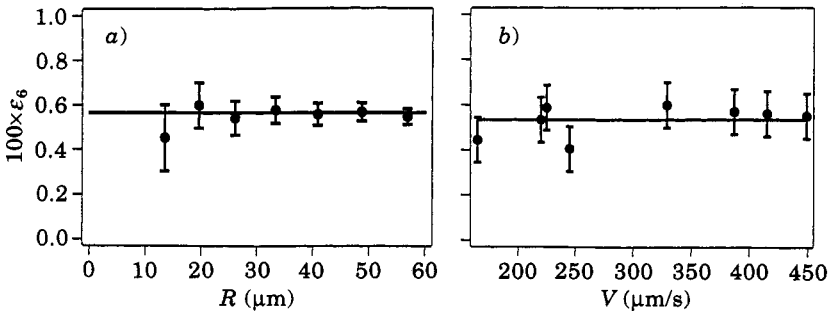


Fig. 5. - a) Relative shape anisotropy ε_6 of a germ as a function of its radius R ($\varepsilon_6 \approx 5.6 \cdot 10^{-3}$); b) ε_6 vs. growth velocity V ($\varepsilon_6 \approx 5.3 \cdot 10^{-3}$).

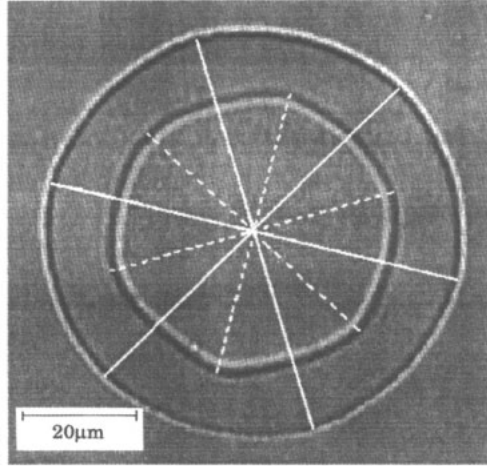


Fig. 6. – Two different shapes of the same germ observed at large and small undercoolings: the bigger germ was grown in the kinetic regime at $\Delta \approx 5$, whereas the smaller one shows the destabilization of the same germ in the dendritic regime at $\Delta \approx 0.3$. The solid lines represent the directions of maximal $\mu(\theta)$, while the dashed lines are those of maximal $\gamma(\theta)$ along which dendrites grow at small undercooling. The directions of maximal $\gamma(\theta)$ and $\mu(\theta)$ do not coincide and clearly form an angle of 30° .

$L \approx 5 \cdot 10^7 \text{ erg/cm}^3$, $\mu \approx 130 \text{ } \mu\text{m/s/}^\circ\text{C}$ and $d < 20 \text{ } \mu\text{m}$, so that $Ld\mu/\kappa$ is less than 0.1. This value is smaller than 1, justifying *a posteriori* the assumption that the latent-heat release is negligible. One can now return to the problem of the absolute restabilization. A linear stability calculation, which neglects latent-heat effects, gives

$$\Delta^* = 1 + \frac{D/d_0}{K\mu T^*}, \quad (5)$$

where $d_0 = \gamma/L \approx 1.3 \text{ \AA}$ is the capillary length, $D \approx 1.2 \cdot 10^{-7} \text{ cm}^2/\text{s}$ the impurity diffusion coefficient in the isotropic liquid, $K \approx 0.33$ the impurity partition coefficient that we assume independent of the front velocity V (experimentally V is always much smaller than $D/\lambda \approx 1 \text{ cm/s}$, where λ is a diffusion jump distance of the order of a molecular distance) and $T^* \approx 359 \text{ K}$ the melting temperature of the pure material. With these values, known generally with an uncertainty of 10%, one calculates $\Delta^* \approx 7 \pm 2.5$. This value is larger but compatible with the experimental one. Indeed, one can show that perturbations have not enough time to grow and become visible through the microscope when the supersaturation is larger than 5. This is due to the finite resolution of the microscope and the finite duration of the experiment.

Another important property of the kinetic-coefficient is its anisotropy. It can be measured from the shape of the germs observed beyond absolute restabilization. Indeed one knows that the growth form obeys Wulff's rule for the kinetic-coefficient diagram [4]. Experimentally, one can measure $R(\theta, t)$ (θ polar angle) and expand it in a Fourier series

$$R(\theta, t) = R_0(t) + \delta_6(t) \cos(6\theta + \phi_6) + \dots \quad (6)$$

According to the Wulff construction, $R_0(t)$ and $\delta_6(t)$ are both proportional to time so that the relative anisotropy $\varepsilon_6 = \delta_6(t)/R_0(t)$ must be constant. We have checked this experimentally by measuring ε_6 as a function of the germ size (fig. 5a): experimentally, the germ form remains similar in time. Furthermore, we have found that ε_6 does not depend on the

supersaturation and the impurity concentration (fig. 5b)). Moreover, it is easy to prove that ε_6 is equal to the relative anisotropy of the kinetic coefficient itself. One can thus write

$$\mu(\theta) = \mu[1 + \varepsilon_6 \cos(6\theta + \phi_6) + \dots] \quad (7)$$

with $\varepsilon_6 \approx 5.6 \cdot 10^{-3}$. One must note that the equality of the ε 's does not apply to higher-order harmonics: thus, for instance, $\varepsilon_{12}^{\text{shape}} \neq \varepsilon_{12}^{\text{kinetic coefficient}}$. These components, which are much smaller than ε_6 , will be given in a more complete publication. Finally, we note that this anisotropy is not very different from that found for the surface energy ($3 \cdot 10^{-3}$) [2].

Let us now discuss the problem of the relative orientation of the directions of maximal $\gamma(\theta)$ and $\mu(\theta)$. Because of the C_{6v} symmetry of our crystal [5], the angle between these two directions may be 0 or $\pi/6$. To obtain this angle, we first grow a germ at large supersaturation in the kinetic regime (fig. 6) we mark the directions of maximal $\mu(\theta)$. Then, we slowly increase the temperature to melt the germ until its radius is close to a few μm . The final temperature is chosen slightly below the liquidus temperature to insure that the germ never disappears completely, thus losing its crystallographic orientation. After about half an hour, the germ is perfectly circular and it is possible to destabilize it in the diffusive regime by decreasing the temperature again (fig. 6). The new temperature is chosen such that the supersaturation is close to 0.3. It is then very easy to locate the directions of dendritic growth corresponding to the maxima of the surface energy $\gamma(\theta)$. This experiment has been performed many times and shows unambiguously that the directions of maximal $\mu(\theta)$ and $\gamma(\theta)$ do not coincide but meet at an angle of 30° . This 30 degree offset has been found by Liu and Goldenfeld in numerical simulations of crystal growth process on a two-dimensional lattice [6].

In order to explain the order of magnitude of the kinetic coefficient, let us write it as [7]

$$\mu = \frac{\beta D_{\text{sd}} L \Omega}{a k_{\text{B}} T^{*2}}. \quad (8)$$

In this formula, D_{sd} is the self-diffusion coefficient of the pure material in the liquid phase, Ω the molecular volume and a some molecular average size which can be defined through Ω as $a \approx (6\Omega/\pi)^{1/3}$. The dimensionless parameter β characterizes the difference between a molecular jump leading to attachment to the solid and the diffusional jump of a molecule in the liquid. To our knowledge, there is no direct measurement of D_{sd} but, for estimation, we can express it through the viscosity η of the liquid via the Einstein relation

$$D_{\text{sd}} = \frac{k_{\text{B}} T}{3\pi a \eta}. \quad (9)$$

This viscosity has been measured in HET and is close to 0.3 poise at the transition temperature T^* [8]. It gives $D_{\text{sd}} \approx 1.2 \cdot 10^{-7} \text{ cm}^2/\text{s}$ by taking $\Omega \approx 1.6 \cdot 10^{-21} \text{ cm}^3$, a value that is very close to that we found for the impurity diffusion coefficient. From these values and using eqs. (8) and (9) we calculate

$$\mu = 3.7 \cdot 10^{-3} \beta \text{ (cm/s/}^\circ\text{C)}. \quad (10)$$

Experimentally, we have measured $\mu \approx 1.3 \cdot 10^{-2} \text{ cm/s/}^\circ\text{C}$, so we can estimate the parameter $\beta \approx 3.5$. This value is reasonable.

In conclusion, we have investigated the fast growth of the impure liquid crystal HET at large supersaturation. We found that the growth rate is linear with undercooling: $V = \mu(T_s - T)$. The kinetic coefficient μ is independent of impurity concentration and equal to

130 $\mu\text{m/s}/^\circ\text{C}$. This value is much smaller than in usual plastic crystals. For instance, Glicksman *et al.* [9] give $\mu \approx 20 \text{ cm/s}/^\circ\text{C}$ for succinonitrile, a value that is three orders of magnitude larger than ours. We believe that this is mainly due to the difference between the diffusion coefficients in both materials. We also measured the anisotropy of the kinetic coefficient and the directions along which its value is maximal. These directions do not coincide with those of maximal surface energy and make an angle of 30° .

* * *

This work was supported by the Centre National d'Etudes Spatiales.

REFERENCES

- [1] OSWALD P., MALTHÊTE J. and PELCÉ P., *J. Phys. (Paris)*, **50** (1989) 2121.
- [2] OSWALD P., *J. Phys. (Paris)*, **49** (1988) 1083.
- [3] GÉMINARD J. C., BECHHOEFER J. and OSWALD P., *J. Cryst. Growth*, **114** (1991) 640.
- [4] CHERNOV A. A., *Sov. Phys. Crystallog.*, **7** (1963) 728.
- [5] OSWALD P., *J. Phys. (Paris) Lett.*, **42** (1981) L-171.
- [6] LIU F. and GOLDENFELD N., *Phys. Rev. A*, **42** (1990) 895.
- [7] CAHN J. W., HILLIG W. B. and SEARS G. W., *Acta Metall.*, **12** (1964) 1421.
- [8] PALIERNE J. F., Thèse 3ème Cycle, Orsay (1983).
- [9] GLICKSMAN M. E., SCHAEFER R. J. and AYERS J. D., *Metal. Trans. A*, **7** (1976) 1747.